IEEE Open Journal of
Antennas and Propagation

Received 19 November 2022; revised 28 December 2022; accepted 28 December 2022. Date of publication 6 January 2023;
date of current version 23 January 2023.

Digital Object Identifier 10.1109/OJAP.2023.3234541

Design of a 2-Bit Reconfigurable UWB Planar Antenna Array for Beam Scanning Application

ZUQI FANG, HANQING YANG, YUAN GAO, FENG ZHAI, JUN WEI WU (Member, IEEE), QIANG CHENG (Senior Member, IEEE), AND TIE JUN CUI (Fellow, IEEE)

State Key Laboratory of Millimeter Waves, Southeast University, Nanjing 210096, China

CORRESPONDING AUTHOR: Q. CHENG (e-mail: qiangcheng@seu.edu.cn)

This work was supported in part by the Basic Scientific Center of Information Metamaterials of the National Natural Science Foundation of China under Grant 6228810001; in part by the National Key Research and Development Program of China under Grant 2017YFA0700201, Grant 2017YFA0700202, Grant 2017YFA0700203, Grant 2018YFA070190, and Grant 2021YFA1401002; in part by the National Natural Science Foundation of China under Grant 62171124, Grant 61631007, Grant 61571117, Grant 61138001, Grant 61371035, Grant 61722106, Grant 61731010, and Grant 11227904; and in part by 111 Project under Grant 111-2-05; in part by the Major Project of Natural Science Foundation of Jiangsu Province under Grant BK20212002; in part by the Fundamental Research Funds for the Central Universities under Grant 2242022R10055; and in part by the Jiangsu Provincial Innovation and Entrepreneurship Doctor Program.

ABSTRACT Reconfigurable antennas have been widely employed for beam scanning in recent years. However, such antennas are usually limited by narrow bandwidth. To overcome this challenge, we present a linearly polarized 2-bit ultra-wideband (UWB) antenna array in C-band. The antenna array consists of 16 Vivaldi elements, 16 wideband phase shifters and a feeding network. The structural symmetry is employed to provide a couple of opposite phase states in the broad bandwidth. The measured results show that the antenna array can operate well in a broad bandwidth from 4.0 to 5.5 GHz (the relative bandwidth $\sim$ 31.5%) with reflection loss lower than -10 dB. The scanning angle ranges from $-45°$to $45°$ with the sidelobe below -10dB, which agrees well with the theoretical predictions. The design features low cost, simple structure, easy fabrication and broad bandwidth.

INDEX TERMS Reconfigurable antenna, 2-bit, beam scanning, antenna array.

I. INTRODUCTION

RECONFIGURABLE antennas can be used in radar, remote sensing, biomedical engineering, satellite and the fifth-generation (5G) communications. Such antennas are able to change their operating frequencies, polarizations, beam widths and directions, thus they are more flexible and cheaper than traditional phase array antennas. Hence, they have attracted extensive attentions of the researchers in radar and wireless communication societies.

Recently, a series of low-cost reconfigurable antennas have been proposed as alternatives of traditional phased arrays for beam scanning. For instance, digital coding metasurface antennas have been employed to implement beam shaping [1], [2], wherein PIN diodes are embedded and utilized to realized 1, 2, or 3-bit discrete phase shifts [3], [4], [5], [6]. Although the gains and sidelobe levels of such antennas suffer inevitable deterioration owing to the phase quantization, they still provide a good route to balance the cost and performance [7]. Varactor diodes can also be employed in reconfigurable antennas such as to achieve continuous phase adjustment [8], [9], [10]. In addition, the MEMS switches [11] and liquid crystals [12] are also promising candidates for reconfigurable antennas.

Reconfigurable beam scanning antennas are usually plagued by narrow bandwidth [13], [14]. It stems from the frequency dispersion of the tunable materials or devices, making it hard to maintain a stable phase response in wide bandwidth [15], [16], [17]. A lot of efforts have been devoted to improve the impedance bandwidth of reconfigurable beam scanning antennas. For instance, the bandwidths in [3] and [17] are extended to 13% and 21.4%, respectively. However, they are still unable to meet the requirements of ultra-wide bandwidth (UWB) applications.

In this paper, we proposed a 2-bit reconfigurable antenna array which features broad bandwidth and flexible beam scanning capability. Due to the structural symmetry, the antenna can provide a couple of stable opposite phase states in the relative bandwidth of 31.5%. The design is verified through full-wave simulations and experiments. The rest of this paper is organized as follows. In Section II, the

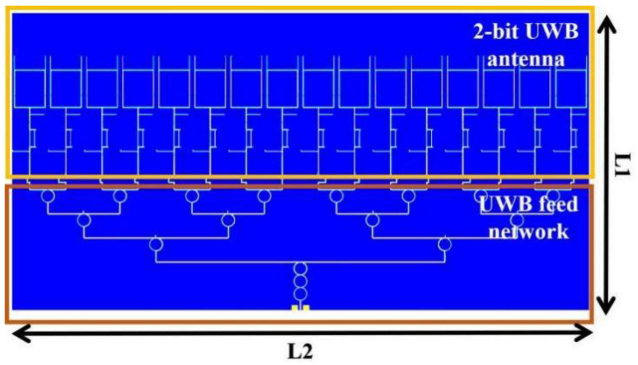

FIGURE 1. The geometry of the designed 2-bit reconfigurable UWB planar antenna array, where L1=205 mm, L2=400 mm.

configuration and design of the proposed 2-bit reconfigurable antenna array are introduced. In Section III, the simulation and experimental results of the fabricated antenna array are given. Finally, Section IV concludes the whole paper.

II. ANTENNA ARRAY DESIGN

A. GENERAL CONFIGURATION

The geometry of the 2-bit reconfigurable antenna array is illustrated in Figure 1. The array consists of Vivaldi antenna elements, 90° phase shifters, and a feeding network, and operates in the C band. The whole size of the array is 400 mm × 205 mm.

The basic 2-bit antenna element is shown in Figure 2, which consists of a Vivaldi antenna element and a 90° phase shifter. As shown in Figure 2(d), two dielectric substrates and three copper layers form the vertical structure of the element. The two dielectric substrates are both Rogers RO4350B ($\varepsilon_r = 3.48$, $\delta = 0.0037$ @10GHz), with the thicknesses of h1=0.25mm and h2=0.53mm, respectively. The three copper layers all have a thickness of 0.035mm. The top copper layer acts as the feeding layer of the antenna. The middle layer is the Vivaldi antenna responsible for energy radiation, and the bottom layer is the control layer for transmitting control signal to antenna elements.

The details of the UWB antenna element and the phase shifter are illustrated in Figure 2, and the geometric dimensions are shown in Table 1. As marked in Figure 2(b), two PIN diodes (BAR64-02EL from Infineon Technologies) named P1 and P2 are placed symmetrically on the feeding layer. The S parameters of the diode, instead of Lumped RLC, are directly imported into CST MWS to characterize its broadband behavior. When one diode is turned on and the other is turned off, a phase shift of 0°or 180°(Case I/II) will be obtained. Therefore, the biasing line on the top of the feeding layer is required to connect the control layer by a via-hole to provide the necessary biasing voltages of the diodes.

The simulated S_{11} parameters of the antenna element under the two states (Case I/II) are presented in Figure 3. Compared to the traditional Vivaldi antenna, the overall

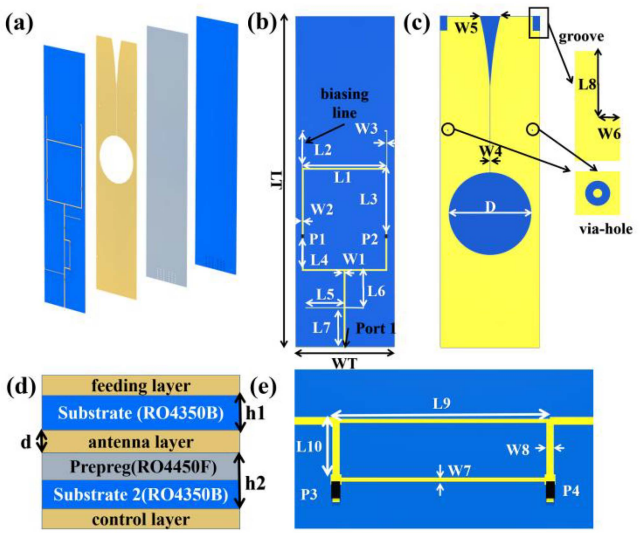

FIGURE 2. Configuration of the 2-bit UWB antenna element. (a) The exploded view. (b) The top copper layer for Vivaldi antenna element. (c) The middle Vivaldi antenna. (d) The side view with of the element. (e) The top copper layer for wideband phase shifter.

TABLE 1. Geometric dimensions of the UWB antenna element.

C	100 pF	L8	3.3mm	W4	0.15mm
L1	21.5mm	L9	12.5mm	W5	5.2mm
L2	9.55mm	L10	3.41mm	W6	0.075mm
L3	17.4mm	D	20.8mm	WT	25mm
L4	8.2mm	W1	0.4mm	LT	83.5mm
L5	9.9mm	W2	0.4mm	W7	0.23mm
L6	9.25mm	W3	0.15mm	W8	0.41mm
L7	10.2mm	d	0.035 mm	h1	0.25 mm
h2	0.53 mm				

impedance bandwidth ($|S_{11}|<-10$ dB) of the antenna element is greatly limited by the feeding layer, but the element can still operate well in the frequency range of 3.9∼5.7 GHz. The relative bandwidth is nearly 38%, indicating that it is suitable for many UWB applications. Although the structural symmetry of the antenna element is employed to provide the 180° wideband phase difference, the accuracy of phase quantization of the antenna element is still insufficient to support good property of array. Hence, a wideband phase shifter is needed to enhance the performance of the antenna element.

B. WIDEBAND PHASE SHIFTER

The wideband phase shifter shown in Figure 2(e) is designed to improve the accuracy of phase quantization by generating 90°phase difference. The dimensions of the directional coupler are carefully optimized to realize the 90°phase difference, which is related to the ON/OFF states (Case III/IV) of the PIN diodes (P3 and P4 are also BAR64-02EL) in Figure 2(e).

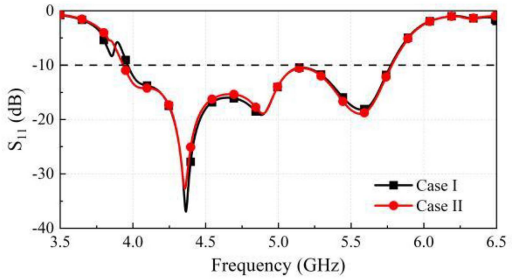

FIGURE 3. The simulated S11 of the UWB antenna element in Case I (P1 is on and P2 is off) and II (P1 is off and P2 is on) without the phase shifter.

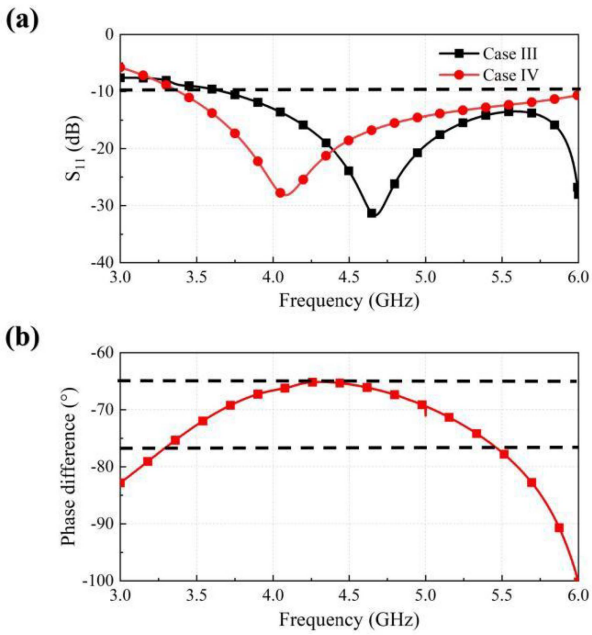

FIGURE 4. (a) S11 curves of the designed 90° phase shifter for Case III (The diodes are turned on) and Case IV (The diodes are turned off). (b) The phase difference between the two cases.

The S_{11} curves of the phase shifter when P3 and P4 are turned on (Case III), or P3 and P4 are turned off (Case IV), are shown in Figure 4(a). They are both below −10 dB from 3.7 GHz to 5.5 GHz, while their phase difference remains between 68°and 82°from 3.7 GHz to 5.5 GHz in Figure 4(b). Because the range of phase shifter is sacrificed to ensure that the impedance bandwidth ($|S_{11}|<-10$ dB) meets the design objective, some corrective measures, such as changing phase coding strategy and adding the pseudo-random phase in initial phase, are employed to adjust the operating situation of the antenna to reduce the impact caused by the limited phase shift range.

C. 2-BIT UWB ELEMENT

Finally, we proceed to investigate the performance of the antenna element when the phase shifter is included, as shown in Figure 2(a). The simulated S_{11} of the 2-bit antenna element with four phase states, generated by the combination of Case I/II and Case III/IV, is presented in Figure 5(a). It

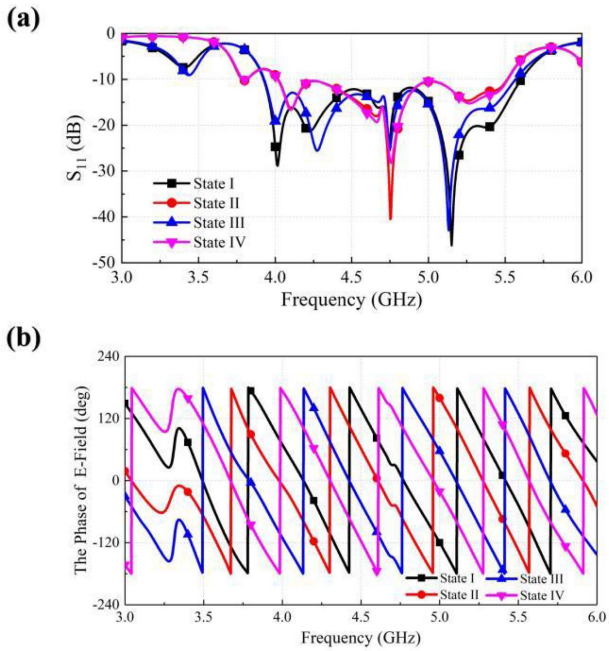

FIGURE 5. (a) S11 of the 2-bit antenna element in four phase states. (b) The phases of the co-polarization electric field measured by the electric-field probe located in the front of the antenna element.

is clear that, with the introduction of the phase shifter, the impedance bandwidth ($|S_{11}|<-10$ dB) of the 2-bit antenna element is slightly narrowed compared to Figure 3, which ranges from 4 GHz to 5.5 GHz with a relative bandwidth of 31%.

Moreover, the simulated phase states of the antenna element measured by the electric-field probe are presented in Figure 5(b). Since the structure of the phase shifter is modified for placing the biasing line, the phase difference of element generated by the phase shifter remains between 80° and 88° from 4 GHz to 5.5 GHz, as shown in Figure 5(b), which is closer to the ideal phase states than the single wideband phase shifter. In summary, the 2-bit antenna element reaches the design targets with excellent performance. Then, a feeding network is required to transmit the microwave signal to the designed elements.

D. FEEDING NETWORK

A feeding network with Taylor weight distribution and −10 dB edge taper is designed to feed the antenna elements. The Wilkinson power splitter is used as the basic structure of the feeding network to improve the isolation between the elements at the same level. Figure 6(a) shows the simulation result of feeding network, wherein the 10 dB return loss bandwidth is above 2.2 GHz and the relative bandwidth is 53%. Moreover, the amplitude distributions fit well with the ideal ones at 4.0 GHz, 4.5 GHz and 5 GHz, respectively, as shown in Figure 6(b). So far, the physical structure design of the antenna has been completed and the phase codes for beam steering are then discussed.

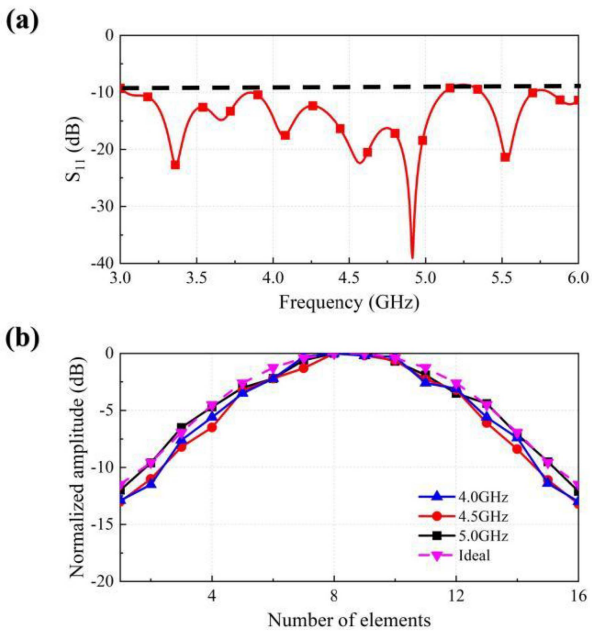

FIGURE 6. (a) The reflection coefficient and (b) the amplitude distribution of the feeding network.

E. PHASE QUANTIZATION

To realize a scanning beam, the phase states of antenna elements should be coded to change the wavefront direction. According to the classical antenna theory, the phases of all elements should be identical for broadside radiation. However, for oblique radiation, different phase codes of antenna elements are required. Moreover, it is necessary to adopt phase quantization because of the finite phase states of the proposed reconfigurable antenna element.

In [19], the round off method for phase coding was investigated to design phased array whose elements had 4 discrete phase states with the resolution of 90°. However, because of the inhomogeneous step of the phase states of the designed 2-bit UWB antenna element, the method are implemented as Table 2, which shows the relation between the phase code and the required continuous phase of the element, and the purpose is to improve the pointing accuracy of antenna array.

Nevertheless, the above coding strategy still results in phase quantization effects [17]. In order to further reduce such errors, one can slightly change the last bit of phase code for n-bit element ($n \geq 2$), since it can break the periodicity of phase quantization error. But the available phase states are actually reduced [20]. Therefore, we still use the round off method for phase quantization in our design. To avoid the high sidelobe level caused by the phase quantization error, an additional pseudorandom phase (PP) is added to the initial discrete phase for each element as shown in Table 3, which breaks the periodicity of phase quantization error [17]. In addition, the additional PP will reduce the influence of the non-homogeneous phase steps.

TABLE 2. Determination the phase code.

Code	00	01	10	11
Phase	0°-80°	80°-180°	180°-260°	260°-360°

TABLE 3. The additional pseudorandom phase of each element at 4.5 GHz.

Element	1	2	3	4	5	6	7	8
PP(°)	-10	-55	-10	-20	-55	-30	-55	0
Element	9	10	11	12	13	14	15	16
PP(°)	-84	-55	-68	-10	-76	-10	-50	-10

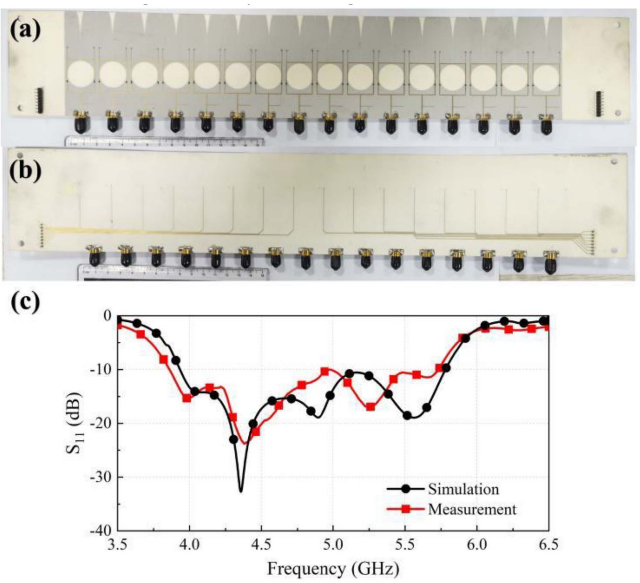

FIGURE 7. (a-b) Top and bottom views of the antenna element without the feeding network. (c) The simulated and measured S11 when only the eighth element on the left of Figure 7(a) is fed.

III. FABRICATION AND MEASUREMENT

To validate our design, the 2-bit antenna array was manufactured and measured. The top and bottom views of the Vivaldi antenna elements without the feeding network and phase shifter are provided in Figure 7(a) and (b). To characterize the radiation property of single element within the array, we only feed the eighth element on the left of Figure 7(a), while the other elements are connected to 50Ω resistors. The measured 10-dB return loss bandwidth is about 1.88 GHz with the relative bandwidth of 39.1%, which is in good agreement with the simulation result.

The fabricated 2-bit reconfigurable antenna array combined with the feeding network is exhibited in Figure 8(a), in which the front view is provided, respectively. The measured reflection coefficient in Figure 8(b) indicates that the −10 dB bandwidth is from 3.8 to 6 GHz (the relative bandwidth is 45%), which is wider than the simulation result. This can be attributed to the power dissipation of the feeding

TABLE 4. Performance comparison of typical reconfigurable antennas.

	Type	Bandwidth	Operating frequency (GHz)	Polarization	Element Number	Bit Width	Scanning range
[2]	RTA	29%	13.5	LP	256	1-bit	±60°
[13]	RRA	10.96%	7.85	LP	n.a.	1-bit	n.a.
[15]	planar antenna	Narrow Band	2	LP	4	1-bit	±30°*
[17]	planar antenna	21%	5.7	LP	16	1-bit	±30°*
this work	planar antenna	31.5%	4.8	LP	16	2-bit	±45°

*Only switchable in few directions

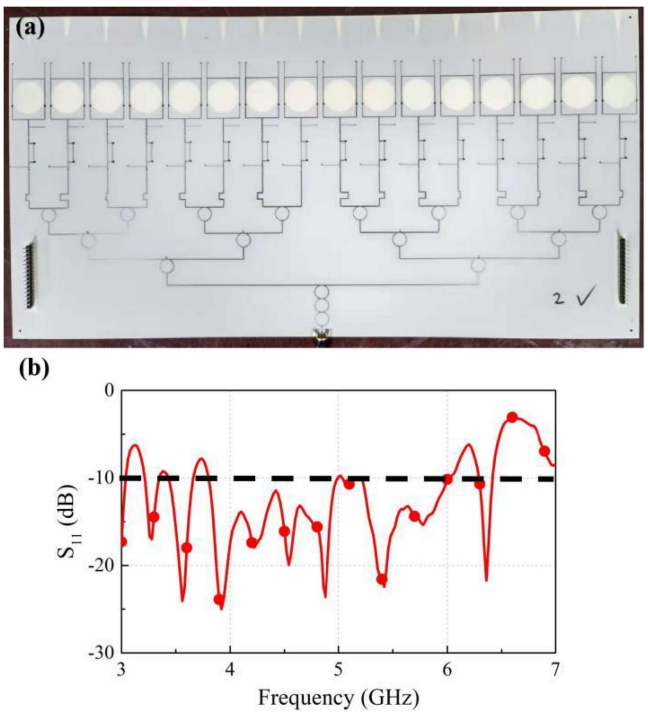

FIGURE 8. (a) Top views of antenna array with the feeding network. (b) The measured S11 of the antenna array when the main lobe direction is normal direction of array.

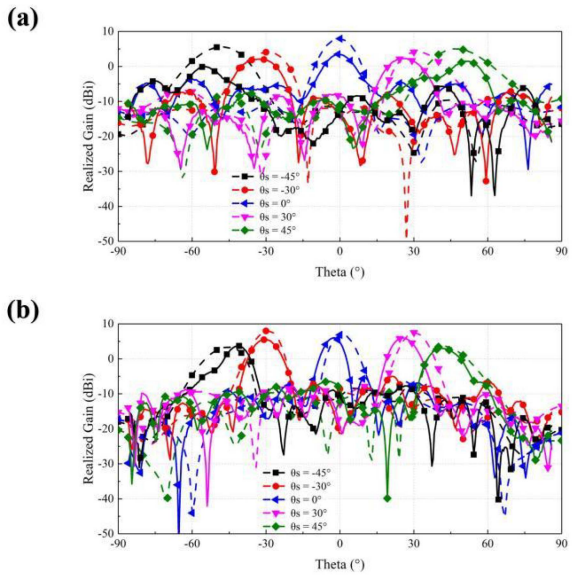

FIGURE 9. The measured (the solid line) and simulated (the dashed line) radiation patterns of the 2-bit antenna array at (a) 4 GHz and (b) 5.5 GHz.

network, which leads to reduced quality factor and expanded impedance bandwidth.

In the end, Figure 9(a) and (b) illustrate the measured and simulated radiation patterns of the fabricated 2-bit antenna array at 4 GHz and 5.5 GHz, respectively. The antenna shows excellent scanning ability from −45°to 45° in the observation bandwidth when we change the phase coding sequence of the elements, and the sidelobe levels remain below −10 dB, generally. For comparison, the simulated radiation patterns of the antenna array are also given in Figure 9(a) and (b), which are consistent with the measurement results except that the maximum antenna gain along broadside is reduced by 2.5 dB at 4 GHz and 1.5 dB at 5.5 GHz. This may be due to the loss in the feeding network being relatively more significant at 4 GHz.

Finally, we summarize performance comparisons among the previously reported reconfigurable antennas and this work in Table 4. It is obvious that the proposed reconfigurable planar antenna array exhibits wide impedance bandwidth and moderate scanning range. Besides, in comparison to RRA (reconfigurable reflectarray antennas) and RTA (Reconfigurable transmitarray antennas), this design has an additional advantage of lower profile, making it easier to be integrated in electronic systems.

IV. CONCLUSION

In this paper, a 2-bit reconfigurable UWB antenna array is proposed. It is composed of Vivaldi antenna elements, 90° UWB phase shifters and a feeding network. The simulated and measure results show that the antenna array can operate well within the bandwidth of 4.0 ∼ 5.5 GHz, with the

sidelobe being lower than -10 dB and the scanning range covering $-45° \sim 45°$. Thanks to the good performance of the antenna array, we believe that it may find potential applications in areas including wireless communications and radar detections.

REFERENCES

[1] T. J. Cui, M. Q. Qi, X. Wan, J. Zhao, and Q. Cheng, "Coding metamaterials, digital metamaterials and programmable metamaterials," *Light Sci. Appl.*, vol. 3, p. e218, Oct. 2014.

[2] Y. Xiao, F. Yang, S. Xu, M. Li, K. Zhu, and H. Sun, "Design and implementation of a wideband 1-bit transmitarray based on a Yagi–Vivaldi unit cell," *IEEE Trans. Antennas Propag.*, vol. 69, no. 7, pp. 4229–4234, Jul. 2021.

[3] P. Liu, Y. Li, and Z. Zhang, "Circularly polarized 2 bit reconfigurable beam-steering antenna array," *IEEE Trans. Antennas Propag.*, vol. 68, no. 3, pp. 2416–2421, Mar. 2020.

[4] X. Li, Z. H. Wu, and Q. Cheng, "A 1-bit reconfigurable antenna in Ku-band," in *Proc. Cross Strait Radio Sci. Wireless Technol. Conf. (CSRSWTC)*, 2021, pp. 7–9.

[5] J. C. Liang et al., "An angle-insensitive 3-bit reconfigurable intelligent surface," *IEEE Trans. Antennas Propag.*, vol. 70, no. 10, pp. 8798–8808, Oct. 2022, doi: 10.1109/TAP.2021.3130108.

[6] X. Yang, S. Xu, F. Yang, and M. Li, "A novel 2-bit reconfigurable reflectarray element for both linear and circular polarizations," in *Proc. IEEE Antennas Propag. Soc. Int. Symp.*, 2017, pp. 2083–2084.

[7] H. Yang et al., "A 1-bit 10×10 reconfigurable reflectarray antenna: Design, optimization, and experiment," *IEEE Trans. Antennas Propag.*, vol. 64, no. 6, pp. 2246–2254, Jun. 2016.

[8] T. Li, H. Zhai, L. Li, and C. Liang, "Frequency-reconfigurable bow-tie antenna with a wide tuning range," *IEEE Antennas Wireless Propag. Lett.*, vol. 13, pp. 1549–1552, 2014.

[9] Y. Tawk, J. Costantine, and C. G. Christodoulou, "A varactor-based reconfigurable filtenna," *IEEE Antennas Wireless Propag. Lett.*, vol. 11, pp. 716–719, 2012.

[10] S. Kausar, A. Kausar, S. Shad, and H. Mehrpouyan, "Electronically controlled unit cell for single layer reconfigurable reflect-array antenna," in *Proc. IEEE Int. Symp. Antennas Propag. North Amer. Radio Sci. Meeting (IEEECONF)*, 2020, pp. 1–2.

[11] A. Zohur, H. Mopidevi, D. Rodrigo, M. Unlu, L. Jofre, and B. A. Cetiner, "RF MEMS reconfigurable two-band antenna," *IEEE Antennas Wireless Propag. Lett.*, vol. 12, pp. 72–75, 2013.

[12] S. Bildik, S. Dieter, C. Fritzsch, W. Menzel, and R. Jakoby, "Reconfigurable folded reflectarray antenna based upon liquid crystal technology," *IEEE Trans. Antennas Propag.*, vol. 63, no. 1, pp. 122–132, Jan. 2015.

[13] D. Wang, Y. Tan, L.-Z. Yin, T.-J. Huang, and P.-K. Liu, "A subwavelength 1-bit broadband reconfigurable reflectarray element based on slotting technology," in *Proc. Int. Appl. Comput. Electromagn. Soc. Symp. China (ACES)*, 2019, pp. 1–2.

[14] H. Yang et al., "A 1600-element dual-frequency electronically reconfigurable reflectarray at X/Ku-band," *IEEE Trans. Antennas Propag.*, vol. 65, no. 6, pp. 3024–3032, Jun. 2017.

[15] S. V. S. Nair and M. J. Ammann, "Reconfigurable antenna with elevation and azimuth beam switching," *IEEE Antennas Wireless Propag. Lett.*, vol. 9, pp. 367–370, 2010.

[16] A. Khidre, F. Yang, and A. Z. Elsherbeni, "Circularly polarized beam-scanning microstrip antenna using a reconfigurable parasitic patch of tunable electrical size," *IEEE Trans. Antennas Propag.*, vol. 63, no. 7, pp. 2858–2866, Jul. 2015.

[17] J. Hu, Z.-C. Hao, and Y. Wang, "A wideband array antenna with 1-bit digital-controllable radiation beams," *IEEE Access*, vol. 6, pp. 10858–10866, 2018.

[18] Y. Chang and B. A. Floyd, "A broadband reflection-type phase shifter achieving uniform phase and amplitude response across 27 to 31 GHz," in *Proc. IEEE BiCMOS Comp. Semicond. Integr. Circuits Technol. Symp. (BCICTS)*, 2019, pp. 1–4.

[19] H. Yang et al., "A study of phase quantization effects for reconfigurable reflectarray antennas," *IEEE Antennas Wireless Propag. Lett.*, vol. 16, pp. 302–305, 2017.

[20] S. Taheri and F. Farzaneh, "New methods of reducing the phase quantization error effects on beam pointing and parasitic side lobe level of the phased array antennas," in *Proc. Asia–Pacif Microw. Conf. (APMC)*, 2006, pp. 2114–2117.